ELSEVIER

Journal of Power Sources 55 (1995) 63–71

JOURNAL OF POWER SOURCES

Characterization by electrochemical impedance spectroscopy of passive layers formed on lead–tin alloys, in tetraborate and sulfuric acid solutions

P. Simon [a], N. Bui [a], N. Pebere [a], F. Dabosi [a], L. Albert [b]

[a] *Ecole Nationale Supérieure de Chimie de Toulouse, Equipe de Métallurgie Physique, Laboratoire des Matériaux URA-CNRS 445, 118 route de Narbonne, 31077 Toulouse, France*

[b] *METALEUROP RECHERCHE, 1 avenue Albert Einstein, 78193 Trappes Cedex, France*

Received 22 October 1994; in revised form 24 November 1994; accepted 26 November 1994

Abstract

Lead–tin alloys (up to 2.5 wt.% Sn) were passivated in de-aerated sodium tetraborate solution (pH = 9.1). Voltammetry measurements showed that alloying tin had the effect of inhibiting the oxidation of lead into PbO or PbO_2, but did not hinder the formation of an intermediate compound, PbO_x. By impedance spectroscopy measurements, it was found that the polarization resistance of the passivated electrodes increased when the alloying tin content increased. Pure lead and Pb–0.5 wt.% Sn alloy exhibited a semi-conducting behaviour, while surface films formed on tin-rich alloys were found more electronically conducting. These features were related to the important enrichment of the passive layers with corrosion-resistant SnO_2. The same alloys were passivated in sulfuric acid solutions in experimental conditions to develop an oxide film under the sulfate layer. It was found that for pure lead and Pb–0.5wt.%Sn, the oxide layer behaved as a semi-conductor. With alloying tin ($\geqslant 1$ wt.%), the composite lead–tin oxide was electronic conducting and non-ionic conducting in a solution of pH = 9.1, but in sulfuric acid tin oxide was unstable and increased the ionic conductivity of the passive layers.

Keywords: Lead alloys; Tin; Passive layers; Sulfuric acid; Sodium tetraborate

1. Introduction

The modern tendency for industry to produce maintenance-free and valve-regulated batteries mandated the use of low-antimony or antimony-free alloys, to minimize gassing and resultant dry-out. Most manufacturers have opted for lead–calcium–tin alloys, but lead–calcium and even pure lead are also being used. Other problems associated with these new alloys then appear: loss of cycling capacity, low charge acceptance and low performances in heavy duty cycle discharged batteries [1,2]. All these phenomena were attributed to the presence of a passivation layer at the grid/sulfate interface at the positive grid [3–5]. This passivation layer has been identified as tetragonal PbO (α-PbO) [1,3]. Due to its poor electronic conductivity, the PbO layer impedes electron transfer, resulting in low charge acceptance, loss of cycling capacity, and low performance of the positive grid in heavy duty cycle discharged batteries [4,5]. The formation of the passivation layer is allowed by the high value of pH at the grid/lead sulfate interface, which is close to 9. The alkalization of the interface is due to the diffusion of OH^- through the sulfate layer, which acts as a semi-permeable membrane [6]. A solution to this passivation problem, as known for several years, consists in alloying tin to lead [7–9]. Tin has the property of thinning the PbO layer [10,11], and increasing its electronic conductivity. But the mechanism of the action of tin is still not well understood.

In a previous paper [12], passive layers on lead–tin alloys were prepared in a 0.1 M $Na_2B_4O_7$ solution (pH = 9.1) by potentiostatic polarization. Electronic conduction of the passive layers was evaluated by measuring the polarization currents of the potassium ferro/ferricyanide redox couple which was added to the solution in the passive potential range. It was found that no electron transfer was observed on passive lead alloyed with less than 0.8 wt.% Sn. Electronic conduction of the passive layers increased sharply when the alloying tin content increased from 0.8 to 1 wt.% Sn, but reached a plateau when higher tin contents were used.

SSDI 0378-7753(94)02175-3

X-ray photoelectron spectroscopy (XPS) analysis of the passive layers formed in 0.1 M $Na_2B_4O_7$ was also carried out to elucidate the relationship between the alloying tin content and the electronic conductivity of the passive layers [13]. The signals of tin, lead and oxygen (main components of the passive films) were depleted in unshifted and shifted signals when the conductivity of the films (evaluated by electrochemical study) became very low. The shifted signals were assumed to have originated from positively charged zones on the surface film due to their low conductivity. The shifting increased when the alloying tin decreased, that is when the film conductivity decreased. The concentration of tin (as compared with lead) in the passive films was greatly increased, up to 44, 28, 14, 13 and 3 wt.%, respectively for 2.5, 1.5, 1.3, 1 and 0.5 wt.% Sn alloys. Semi-quantitative analysis showed that one of the effects of alloying tin could be the thinning of the passive films, as observed for Pb–2.5wt.%Sn alloy. The inner layer of the passive films was found to be rich in conducting tin oxide and metallic lead. XPS did not distinguish SnO from SnO_2 signals, but SnO_2 was assumed to be present in the passive films, for reasons of its thermodynamic stability.

Buchanan et al. [14] have already noted the similarity of the anodic behaviour of lead in tetraborate as well as in sulfuric acid solutions in the passive potential range. On the basis of previous results [12,13], this study aims to interpret the electrochemical behaviour of lead and lead–tin alloys in a 1 M H_2SO_4 solution. Due to the duplex $Pb/PbO/PbSO_4$ structure of the lead electrode, it was difficult to use the previous redox couple to characterize the influence of alloying tin. Then, the electrochemical impedance analysis of the $Pb/PbO/PbSO_4$ electrode in 1 M H_2SO_4 was carried out, after 40 h of polarization at +400 mV versus SSE (saturated sulfate electrode). For comparison, the electrochemical impedance spectroscopy (EIS) of the Pb/PbO electrode in a 0.1 M $Na_2B_4O_7$ (pH = 9.1) solution was also analysed.

2. Experimental

The preparation of the lead–tin alloys (0.5, 1, 1.3, 1.5 and 2.5 wt.% Sn) and the electrochemical equipment has been described in previous papers [12,13]. Working electrodes were of a lead–tin alloy with an exposed surface area of 1.3 cm^2. For the cyclic voltammetry measurements in a 0.1 M $Na_2B_4O_7$ solution, the scan rate was 10 mV s^{-1}. The reference electrode used was a Hg/Hg_2SO_4/saturated K_2SO_4, or SSE (saturated sulfate electrode, +642 mV/NHE). All the potentials quoted in this study are referred to this electrode.

For EIS measurements in 0.1 M $Na_2B_4O_7$ solution, the electrodes were polarized at 0 V/SSE, until a steady-state passive current was attained (around 20 h). In a 1 M sulfuric acid solution, the electrodes were polarized at +400 mV/SSE, until a relatively constant-current value was attained, after 40 h. The solutions were constantly stirred during each experiment.

The EIS apparatus consisted of a Solartron Schlumberger 1250 frequency response analyser and a Solartron 1286 electrochemical interface. The data were processed on a Hewlett-Packard 9000 computer.

3. Results and discussion

3.1. Electrochemical behaviour of lead–tin alloys in 0.1 M $Na_2B_4O_7$ solution

Fig. 1 shows a cyclic voltammogram of pure lead and lead–tin alloys in a 0.1 M $Na_2B_4O_7$ solution. For pure lead, three anodic peaks denoted as (A), (B) and (C) can be observed, beginning respectively at about −1000, −920 and +350 mV, two small cathodic peaks (D_1) and (D_2), beginning respectively at about 200 and −125 mV, and a large cathodic peak (E), beginning at about −920 mV.

Peak (A) is associated with the formation of $Pb(OH)_2$ [15]. Peak (B) is related to the oxidation of Pb into PbO, the equilibrium potential of which is −922 mV at pH = 9.1 [16]. This reaction occurred with a release of protons which lowered the pH at the electrode surface and increased the dissolution of Pb into Pb^{2+}. When the PbO layer was thick enough, the oxidation rate decreased, due to the insulating properties of PbO.

The polarization curve of a pure-tin electrode in a 0.1 M $Na_2B_4O_7$ solution can be seen in Fig. 2. According to Pourbaix [16], in a pH = 9.1 solution, the only ther-

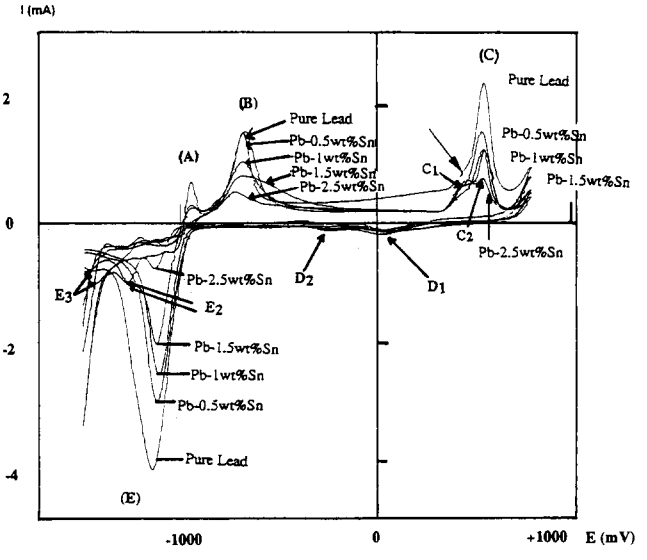

Fig. 1. Cyclic voltammogram of pure lead and different lead–tin alloys, in 0.1 M $Na_2B_4O_7$ solution; scan rate = 10 mV s^{-1}.

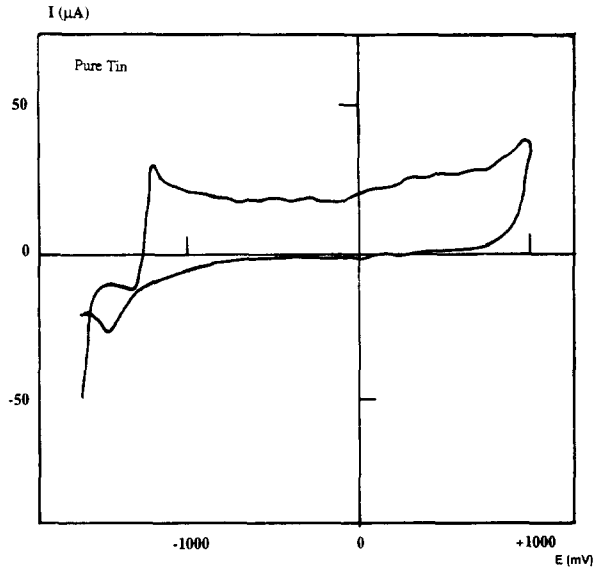

Fig. 2. Cyclic voltammogram of pure tin in 0.1 M $Na_2B_4O_7$ solution; scan rate = 10 mV s^{-1}.

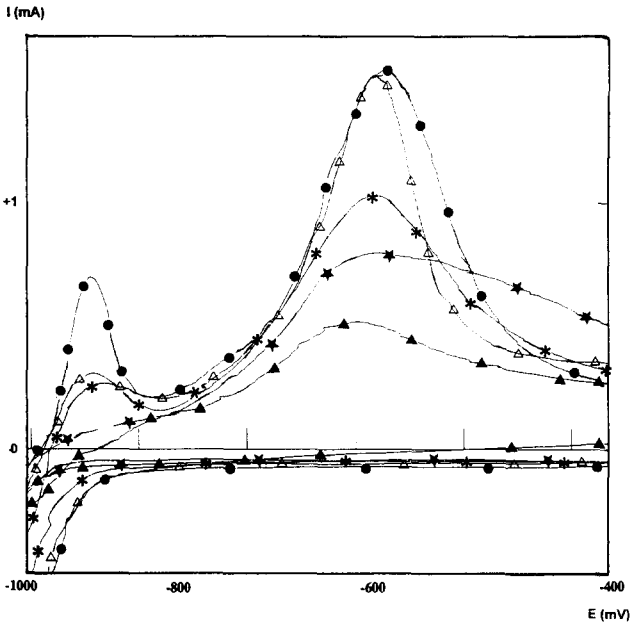

Fig. 3. Magnification of the anodic peaks (A) and (B) of pure lead, and various lead–tin alloys in 0.1 M $Na_2B_4O_7$ solution; scan rate = 10 mV/s^{-1}. (●) pure lead; (△) Pb–0.5wt.%Sn; (*) Pb–1wt.%Sn; (⋆) Pb–1.5wt.%Sn, and (▲) Pb–2.5wt.%Sn.

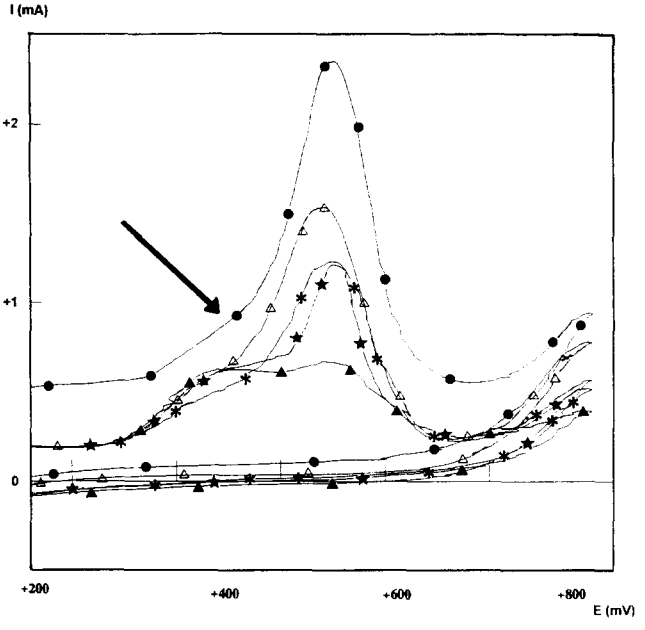

Fig. 4. Magnification of the anodic peak (C) of pure lead and various lead–tin alloys, in 0.1 M $Na_2B_4O_7$ solution; scan rate = 10 mV s^{-1}. (●) pure lead; (△) Pb–0.5wt.%Sn; (*) Pb–1wt.%Sn; (⋆) Pb–1.5wt.%Sn, and (▲) Pb–2.5wt.%Sn.

modynamically stable oxide which can be formed on tin is SnO_2. The equilibrium potential of the Sn/SnO_2 couple is −1285 mV/SSE. From Fig. 2 it appears that the oxidation of pure tin in a 0.1 M $Na_2B_4O_7$ solution took place at −1270 mV. This value is in good agreement with the equilibrium potential of the Sn/SnO_2 couple. After the SnO_2 formation, the current increases very slightly. At the end of the anodic scan, the current increase indicates the beginning of the oxygen-release reaction. On the reverse scan, only one cathodic peak is visible, beginning at −1280 mV, which corresponds to the beginning of the reduction of SnO_2 into metallic tin at pH = 9.1 [11].

Fig. 3 represents the enlarged anodic peaks (A) and (B) of pure lead, and lead–tin alloys 0.5, 1, 1.5 and 2.5 wt.% Sn in a 0.1 M $Na_2B_4O_7$ solution. It can be seen that the intensity of peak (A), which was attributed to the formation of $Pb(OH)_2$ [15], decreases as the tin content in the alloys increases. For Pb–1.5wt.%Sn and Pb–2.5wt.%Sn, the peak is greatly reduced. The same observation can be made with peak (B) related to the formation of lead oxide, namely PbO. The higher the tin content in the alloys, the less lead oxide is formed. Here, it can be concluded that tin inhibits the oxidation of Pb into Pb^{2+}. As the electronic conduction of this oxide was shown to be largely enhanced by the presence of SnO_2 in a high concentration [12,13], it can be assumed that a mixed or composite lead–tin oxide was present on the alloy surface.

An expansion of the anodic peak (C) is shown in Fig. 4. Its intensity decreases with the alloying tin content. For the Pb–2.5wt.%Sn alloy, peak (C) is obviously composed of two peaks (C_1) and (C_2). Peak (C_1) does not seem to appear only on lead–tin alloys. With pure lead, it is possible to see a shoulder on peak (C), marked with an arrow. As the global intensity of peak (C) decreases with an increasing alloying tin content, the shoulder becomes more and more defined. Peak (C_2) is likely associated with the formation of α-PbO_2, the only stable oxide which can form in an alkaline solution [14]. Here again, the inhibition of the formation of PbO_2 by alloying with tin is to be noted.

It is possible that there was formation of high-valency mixed lead–tin oxide, as suggested by Pavlov et al. [17], and Bojinov et al. [18]. Peak (C_1) can be related to the formation of PbO_x ($1 < x \leqslant 1.5$) [9,17–19] through various lead oxidation states, for example $+2.67(Pb_3O_4) + 3(Pb_2O_3)$ with a large overpotential due to a decrease of the surface pH, resulting from the release of protons during anodic reactions.

During the reverse scan of the voltammogram, two small cathodic peaks (D_1) and (D_2) can be observed (Fig. 1). These peaks are thought to correspond to the partial reductions of PbO_2 into PbO_x and PbO_x into PbO, respectively. PbO_x could be Pb_3O_4, since the redox potentials of PbO_2/Pb_3O_4 and Pb_3O_4/PbO are respectively +54 and −215 mV, values not far from peak potentials (D_1) and (D_2). The non-conducting property of the PbO layer is thought to be responsible for the slowing down of the reduction rate. The cathodic peak (E) on pure lead is assumed to come from the reduction of the rest of PbO, PbO_x and PbO_2. It can be seen that peak (E) decreases as the tin level in the alloys increase. This behaviour supports the role of tin in the inhibition of the formation of PbO and PbO_2. As the tin level increases, peak (E_2) becomes more defined. This peak may be related to the reduction of the rest of PbO_x. Peak (E_3) is obviously connected to the reduction of SnO_2 into Sn, as can be seen on the voltammogram of pure tin (Fig. 2).

3.2. Electrochemical impedance spectroscopy of lead–tin alloys in 0.1 M $Na_2B_4O_7$ solution

Pure lead, pure tin and lead–tin alloys were polarized in a 0.1 M $Na_2B_4O_7$ solution at 0 V/SSE in the passivity domain. Impedance measurements were carried out after a constant current was obtained, that is between 15 and 24 h (depending on the alloy composition).

Fig. 5 shows the Nyquist plot obtained for the different lead–tin alloys, pure tin and pure lead. For pure tin and the various lead–tin alloys, diffusion control is observed at low frequencies. For pure lead and Pb–0.5wt.%Sn alloy, the complex plane plot follows a semicircle which can be described, in a first approach, by an equivalent circuit made up of a polarization resistance, R_p, in parallel to a double-layer capacitance, C_{dl}. In this case, R_p, described as the impedance value when the frequency tends to zero, is considered to be equal to the charge-transfer resistance, R_{ct}, which can be obtained by extrapolation of the semicircle toward the real axis. For the other lead–tin alloys, a Warburg-type impedance must be considered and added in series with R_{ct}. The diffusion control seems to be associated with the presence of tin oxide in the corrosion layers. The charge-transfer resistance, R_{ct}, increases when the alloying tin content is increased. The dependence of the values of R_p versus the tin content in the alloys

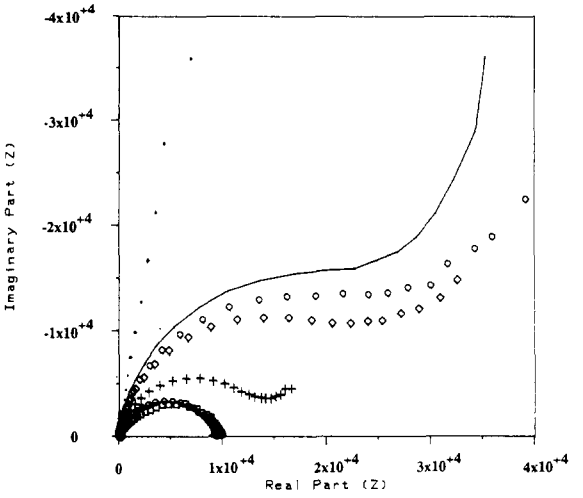

Fig. 5. Nyquist plots for pure tin, pure lead and various lead–tin alloys, after polarization in a 0.1 M $Na_2B_4O_7$ solution at 0 V. (□) Pure lead; (⊖) Pb–0.5wt.%Sn; (+) Pb–1wt.%Sn; (◇) Pb–1.3wt.%Sn; (○) Pb–1.5wt.%Sn; (—) Pb–2.5wt.%Sn, and (●) pure tin.

is in good agreement with the previous electrochemical study [12].

A Bode plot of the impedance is represented in Fig. 6(a) and (b), showing the dependence of the modulus and the phase versus frequency, respectively. At high frequencies, the modulus for the different lead–tin alloys and pure tin appeared to be independent of the frequency, except for pure lead and the Pb–0.5wt.%Sn alloy, and tends to a constant value of the electrolytic resistance, R_e. However, the modulus of pure lead and the Pb–0.5wt.%Sn alloy is one order of magnitude higher than for the other lead–tin alloys studied. In the previous electrochemical study [12], it was shown that passive layers formed on lead–tin alloys with a tin content higher than 0.8 wt.% exhibited good electronic conductivity while the passive layers formed on pure lead and Pb–0.5wt.%Sn were more resistive. The high values of the modulus at high frequency for pure lead and Pb–0.5wt.%Sn alloy confirm the previous results in the sense that alloying with tin improves the electronic conduction of the passive layers. At low frequencies, on the contrary, it can be seen that the impedance modulus of pure lead and low-tin alloys is lower than for high-tin alloys. This behaviour indicates that the polarization resistance R_p of tin-rich alloys is higher than for pure lead and low-tin alloys, in agreement with their higher corrosion resistance found previously [12].

The phase versus frequency plots (Fig. 6(b)) show a marked difference in the impedance characteristics of low-tin and high-tin alloys. At high frequencies, the high value of the phase angle of lead and Pb–0.5wt.%Sn alloy may be explained by the semi-conducting properties of the PbO layer [20]. To interpret this impedance behaviour of lead, the equivalent circuit generally used

Table 1
Fitted parameters of the equivalent circuit shown in Fig. 7, obtained with the 'Simplex' computing program

	C_{sc} (F)	R_{ss} (Ω)	C_{ss} (F)	R_{ct} (Ω)	C_{dl} (F)	CPE_1	CPE_2	R_e (Ω)	Fitting correction
Pure lead	3×10^{-8}	220	1.5×10^{-9}	10300	3×10^{-6}	0.63	0.65	22	0.9996
Pb–0.5wt.%Sn	2×10^{-8}	78	8×10^{-8}	9000	9×10^{-6}	0.83	0.60	21	0.9993

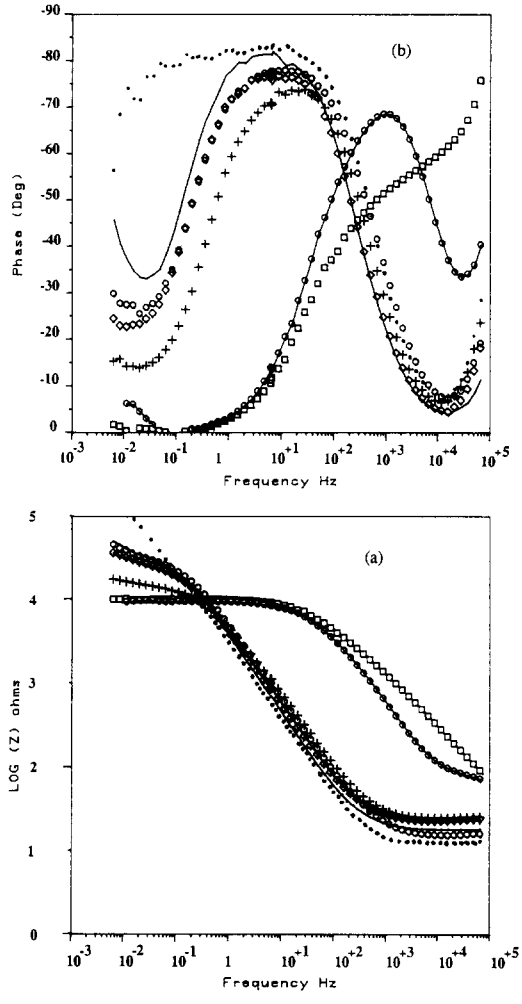

Fig. 6. Bode plots for pure tin, pure lead and the various lead–tin alloys, after polarization in a 0.1 M $Na_2B_4O_7$ solution at 0 V: (a) modulus vs. frequency plot, and (b) phase versus frequency plot. (□) Pure lead; (⊖) Pb–0.5wt.%Sn; (+) Pb–1wt.%Sn; (◈) Pb–1.3wt.%Sn; (○) Pb–1.5wt.%Sn; (—) Pb–2.5wt.%Sn, and (●) pure tin.

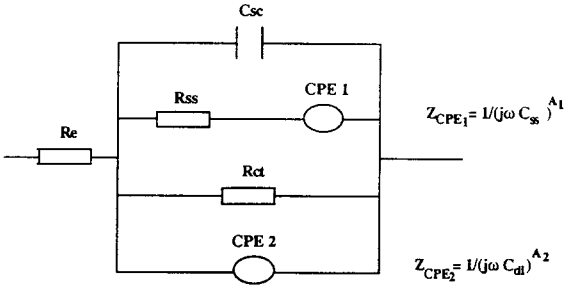

Fig. 7. Proposed equivalent circuit for a pure-lead electrode in a 0.1 M $Na_2B_4O_7$ solution. R_e = resistance of electrolyte; C_{sc} = space charge capacitance; R_{ss} = surface state resistance; C_{ss} = capacitance relative to the storage of the charge on the surface states; R_{ct} = charge-transfer resistance; C_{dl} = double-layer capacitance, and CPE = constant phase element.

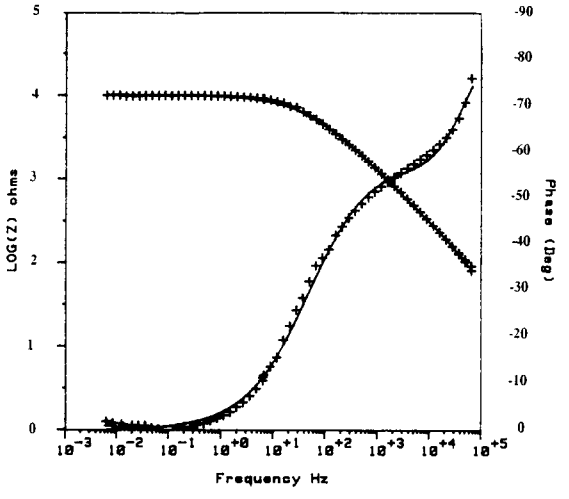

Fig. 8. (– – –) Calculated and (+ +) experimental phase and modulus vs. frequency plots for pure lead in a 0.1 M $Na_2B_4O_7$ solution, using the equivalent circuit shown in Fig. 7.

for semi-conductors was applied [21] with the addition of a constant phase element (CPE_1) [22] to account for the frequency dispersion, and a parallel (CPE_2) to account for the PbO/electrolyte interface (Fig. 7). The best-fit values of the equivalent circuit using the 'Simplex'-fitting procedure are listed in Table 1. An example of the calculated phase versus frequency plot is shown in Fig. 8.

For tin-rich alloys, the surface film is composed of a mixed or composite lead–tin oxide, which is electronically conducting. Their impedance can be described by a simpler equivalent circuit (Fig. 9) where a diffusional impedance Z_D is added to account for the ionic diffusion through the surface film. The best fit parameters are listed in Table 2, where the diffusion resistance R_D is the value of Z_D extrapolated to the real axis for $\omega \rightarrow 0$. It can be seen that R_D increases when the tin content in the alloy increases. An example of the calculated phase and modulus is shown in Fig. 10.

Table 2
Fitted parameters of the equivalent circuit shown in Fig. 9, obtained with the 'Simplex' computing program

Alloy	C_{dl} (F)	R_{ct} (Ω)	R_e (Ω)	CPE	R_D (kΩ)	Fitting correction
Pb–1wt.%Sn	7×10^{-6}	13000	23	0.86	10.5	0.9998
Pb–1.3wt.%Sn	1×10^{-6}	23600	22	0.88	36.5	0.9998
Pb–1.5wt.%Sn	10×10^{-6}	27200	16	0.88	57.8	0.9997
Pb–2.5wt.%Sn	20×10^{-6}	28600	18	0.92	98.5	0.9991

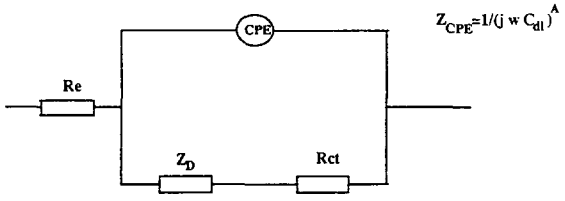

Fig. 9. Proposed equivalent circuit for lead–tin alloys (≥1 wt.% Sn), after polarization in a 0.1 M $Na_2B_4O_7$ solution; Z_d = diffusion impedance.

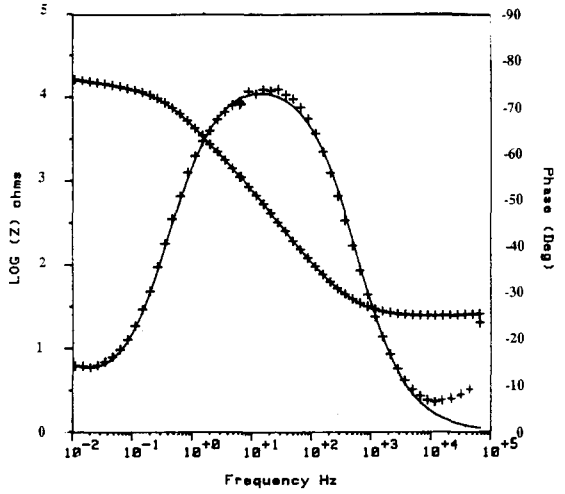

Fig. 10. (– – –) Calculated and (+ +) experimental phase and modulus vs. frequency plot for Pb–1wt.%Sn in a 0.1 M $Na_2B_4O_7$ solution, using equivalent circuit shown in Fig. 9.

The electrochemical impedance behaviour may then be interpreted by the high polarization resistance, the high capacitance of tin-rich alloys, the passive layers of which was enriched with corrosion resistant SnO_2 as shown in previous studies [12,13]. In other words, SnO_2 may be considered as a barrier for ionic conduction through the passive film, increasing the electrochemical impedance which translates the resistance to ionic exchange at the electrode/electrolyte interface, at low frequencies.

This EIS study of the alloy/passive layer electrode in solution at pH 9.1 confirms previous results obtained by electrochemical and XPS analyses, and shows that the role of tin, in the form of SnO_2, consists of changing the semi-conducting properties of the PbO layer which becomes more electronically conductive.

3.3. Electrochemical impedance spectroscopy of lead–tin alloys in 1 M H_2SO_4 solution

Lead–tin alloys and pure lead were polarized in a 1 M H_2SO_4 solution. The potential scan began at −1500 mV at a rate of 1 mV s^{-1}. The electrodes were then held at +400 mV for 40 h. In these conditions, the pure-lead electrode can be described as the Pb/PbO/$PbSO_4$ duplex system. A steady-state passive current was obtained, and the EIS measurements were then carried out. Fig. 11 represents the Nyquist plots for the lead–tin alloys and pure lead. The variation of the cell impedance with frequency follows a semi-circle for pure lead as well for the lead–tin alloys. It appears that control of charged species by diffusion was absent. The polarization resistance R_p (or the charge-transfer resistance R_{ct}) determined from the intercept of the semi-circle with the real part of the cell impedance at low frequencies, decreases when the tin content of the alloys decreases. These results are different from those obtained in a pH = 9.1 solution, where ionic diffusion control was clearly observed, and it was shown that tin has the property of increasing the corrosion resistance of the alloys. But Fig. 11 shows that the corrosion resistance of the alloys in 1 M H_2SO_4 decreases, that is to say, the dissolution rate of the alloys increases, when the tin content increases. This behaviour can be explained by the facility of tin to dissolve in sulfuric acid through the passive layer, as shown by the ring-

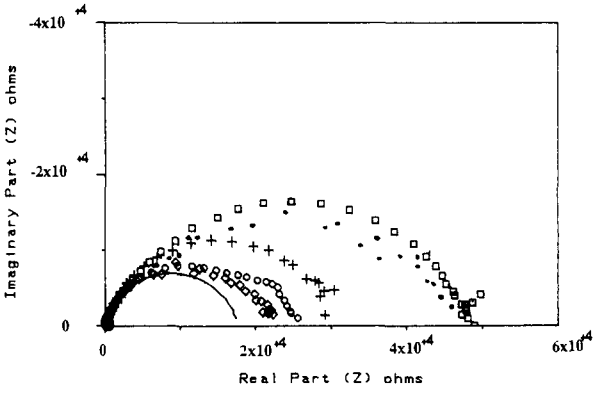

Fig. 11. Nyquist plots for pure lead and various lead–tin alloys, after 40 h polarization in a 1 M H_2SO_4 solution at +400 mV. (□) pure lead; (●) Pb–0.5wt.%Sn; (+) Pb–1wt.%Sn; (◇) Pb–1.2wt.Sn; (○) Pb–1.5wt.%Sn, and (—) Pb–2.5wt.%Sn.

Table 3
Fitted parameters of the equivalent circuit presented in Fig. 7, obtained with the 'Simplex' computing program, for a pure-lead electrode in 1 M H_2SO_4

	C_{sc} (F)	R_{ss} (Ω)	C_{ss} (F)	R_{ct} (Ω)	C_{dl} (F)	CPE_1	CPE_2	R_e (Ω)	Fitting correction
Pure lead	5×10^{-8}	190	2×10^{-9}	51300	2×10^{-6}	0.68	0.88	0.2	0.9999
Pb–0.5wt.%Sn	7×10^{-8}	25	5×10^{-9}	51000	2×10^{-6}	0.65	0.92	0.3	0.9993

disc measurements of Bojinov et al. [18]. As the corrosion rate was purely activation-controlled, the polarization resistance for pure lead was the highest for reasons of the presence of the passive PbO layer underneath the sulfate layer. This PbO layer was shown [12,13] to become thinner and more electronically conductive when the tin level in the alloy increased. This property may explain the decrease of the activation energy controlling the dissolution kinetics of the alloys. In other words, the decrease of the polarization resistance is connected to the increase of the tin content. These impedance results may find confirmation in the works of several authors [9,23], who have shown an increase of the passive current density measured in the potential range of the PbO formation in H_2SO_4.

The modulus and the phase angle versus frequency plots of the cell impedance are presented in Fig. 12. The modulus obtained for pure lead and Pb–0.5wt.%Sn alloy is one order of magnitude higher, at high frequencies, than for the other alloys. As only the effect of the solution and film resistance can be seen at high frequencies, it can be stated that the passive layers formed on lead–tin alloys (with a minimum tin content of 1 wt.% Sn) are much more conductive than those of Pb–0.5wt.%Sn alloy and pure lead. The PbO layer underneath the sulfate layer was shown to have semi-conducting properties [17,20,24]. The duplex structure $PbO/PbSO_4$ of the passive films formed on pure lead and Pb–0.5wt.%Sn alloy can be described by the previous equivalent circuit used for semi-conductors in which the capacitance, C_{dl}, is now related to the sulfate/electrolyte interface. The best-fit parameters are listed in Table 3. An example of the calculated phase and modulus versus frequency plots is given in Fig. 13.

For high-tin alloys, the inner layer is highly conductive due to the presence of tin [12,13]. The simulation of the experimental results can be performed now with a simpler equivalent circuit composed of a parallel combination of R_{ct} and C_{dl} representing the sulfate layer, in series with another parallel R_1–C_1 combination, to take account of the conducting inner layer (Fig. 14). It can be seen in Table 4 that R_1 is quite small, and the contribution of this layer to the electrode impedance is negligible. An example of the calculated phase and modulus versus frequency plots is shown in Fig. 15.

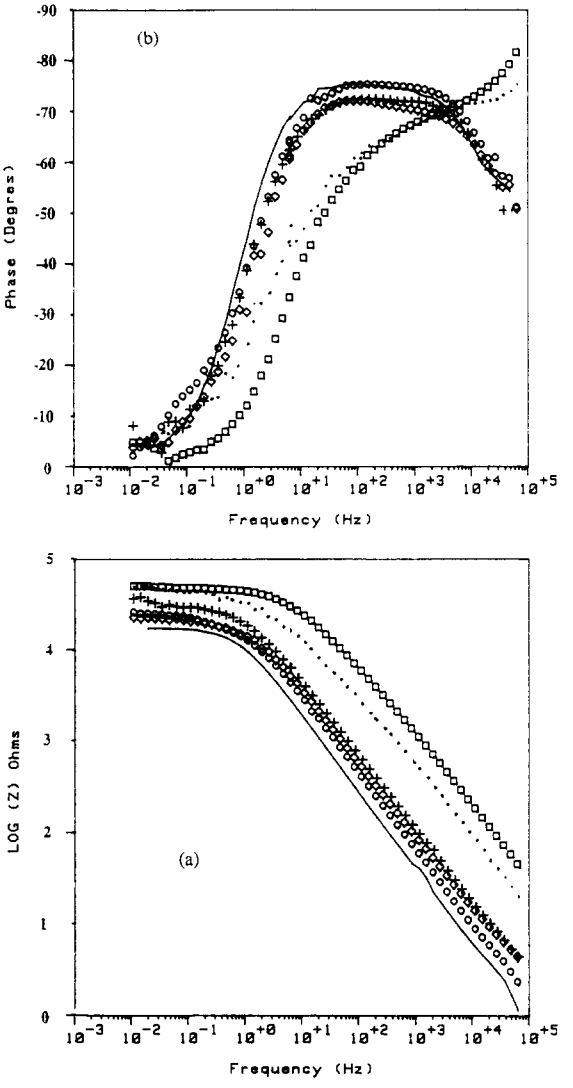

Fig. 12. Bode plots for pure lead and various lead–tin alloys, after 40 h polarization in a 1 M H_2SO_4 solution at +400 mV: (a) modulus vs. frequency plot, and (b) phase vs. frequency plot. (□) pure lead; (●) Pb–0.5wt.%Sn; (+) Pb–1wt.%Sn; (◇) Pb–1.3wt.%Sn; (○) Pb–1.5wt.%Sn, and (——) Pb–2.5wt.%Sn.

The frequency dependence of the phase angle of pure lead and Pb–0.5wt.%Sn at high frequencies exhibit the same features in 1 M H_2SO_4 as in 0.1 M $Na_2B_4O_7$ solutions. However, at high frequencies, up to 10^5 Hz, the high values of the phase angle of lead and Pb–0.5wt.%Sn alloy electrodes cannot be explained by the

Table 4
Fitted parameters of the equivalent circuit shown in Fig. 14, obtained with the 'Simplex' computing program, for lead–tin alloys in 1 M H_2SO_4

Alloy	R_e (Ω)	R_1 (Ω)	C_1 (F)	R_{ct} (Ω)	C_{dl} (F)	CPE_1	CPE_2	Fitting correction
Pb–1wt.%Sn	0.2	2.1	1×10^{-7}	30600	5×10^{-7}	0.73	0.80	0.9997
Pb–1.3wt.%Sn	0.2	2.7	3×10^{-7}	20700	6×10^{-7}	0.66	0.81	0.9998
Pb–1.5wt.%Sn	0.3	1.5	6×10^{-7}	20800	1.2×10^{-6}	0.71	0.84	0.9999
Pb–2.5wt.%Sn	0.2	1.5	1.2×10^{-6}	17500	2.3×10^{-6}	0.75	0.85	0.9999

values of their polarization resistance which are higher than those of high-tin alloys, but may be interpreted by the presence of a semi-conducting PbO layer underneath the $PbSO_4$ layer, and a low value of the capacitance due to the thickness of the layer.

At low frequencies, the phase angles of the different electrodes tend to zero. This means that no diffusion control occurred, unlike in the previous observations in 0.1 M $Na_2B_4O_7$. To explain these features, it is reasonable to state that passivation did not really happen in sulfuric acid solution, as it is known that tin dissolves in this medium [18]. Even with the increase of the pH, due to OH^- diffusion through the sulfate layer, the presence of SO_4^{2-} and adsorbed tin ions in the PbO layer could induce more ionic conduction. This is the reason why the observed polarization resistance decreased when the tin content in the alloys increased. This explanation is in agreement with the work of Pavlov et al. [17] who stated that the PbO layer was no longer passive when tin ions, under the Sn^{2+}, Sn^{3+} or Sn^{4+} state, were adsorbed in the layer.

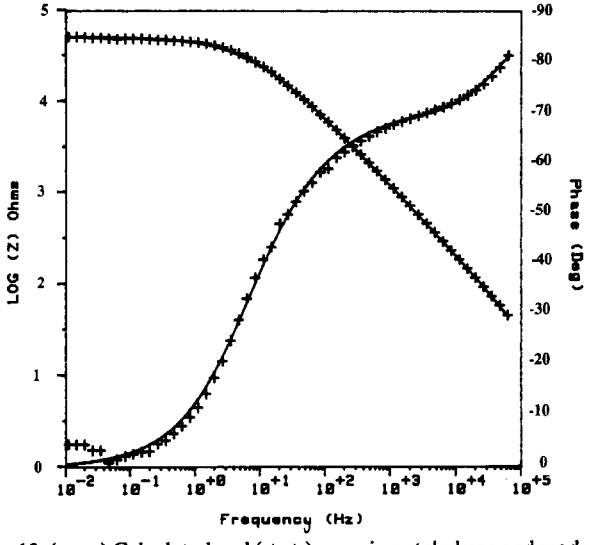

Fig. 13. (– – –) Calculated and (+ +) experimental phase and modulus vs. frequency plot for pure lead in a 1 M H_2SO_4 solution, using the equivalent circuit shown in Fig. 7.

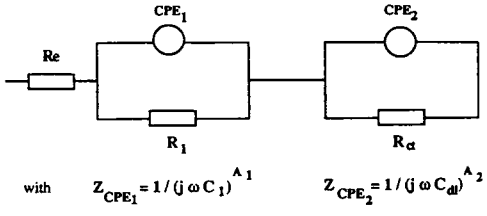

Fig. 14. Proposed equivalent circuit for the lead–tin alloys in a 1 M H_2SO_4 solution. R_{ct} = charge-transfer resistance at the $PbSO_4$/H_2SO_4 interface; C_{dl} = capacitance of the $PbSO_4/H_2SO_4$ interface; R_1 = resistance of the inner layer; C_1 = capacitance of the inner layer, and R_e = resistance of the electrolyte.

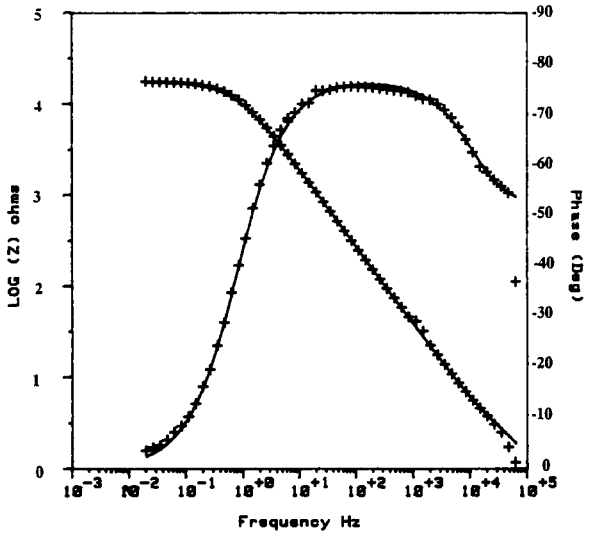

Fig. 15. (– – –) Calculated and (+ +) experimental phase and modulus vs. frequency plot for Pb–2.5wt.%Sn in a 1 M H_2SO_4 solution, using equivalent circuit shown in Fig. 14.

The same study was carried out in a 5 M H_2SO_4 solution. The EIS spectra obtained after 40 h of polarization at 400 mV present the same features as in 1 M H_2SO_4, with a similar effect of alloying with tin on the polarization resistance, the modulus and the phase angle of the electrode impedance. The change in acid concentration did not lead to a difference in the behaviour of the alloys under passivation treatment.

4. Conclusions

This electrochemical impedance study of the effect of alloying tin on the passive layers formed on lead–tin alloys in two different media, 0.1 M $Na_2B_4O_7$ (pH = 9.1) and 1 M H_2SO_4 has led to the following conclusions.

(i) Alloying tin has the effect of inhibiting the oxidation of lead into PbO and PbO_2 in a $Na_2B_4O_7$ solution, but does not seems to hinder the formation of an intermediate compound, PbO_x.

(ii) The polarization resistance of the passivated electrodes increases in the $Na_2B_4O_7$ solution when the alloying tin content increases, but decreases in a H_2SO_4 solution.

(iii) The electrochemical behaviour of lead and lead–tin alloys can be fully described by an equivalent circuit comprising a combination of elements representing a semi-conducting electrode when the alloying tin content is less than 1 wt.%Sn. This simulation shows that tin has the effect of transforming the semi-conducting lead oxide layer into a highly conductive layer.

(iv) Tin oxide is stable in solutions at pH = 9.1, increases the electronic conductivity and decreases the ionic conductivity of the mixed lead–tin oxide. On the other hand, tin oxide is unstable in sulfuric acid and increases the ionic conductivity of the passive layer.

References

[1] J. Burbank, *J. Electrochem. Soc., 106* (1959) 369.
[2] J. Lander, *J. Electrochem. Soc., 98* (1951) 213.
[3] D. Pavlov, C.N. Poulieff, E. Klaja and N. Iordanov, *J. Electrochem. Soc., 116* (1969) 316.
[4] P. Rüetschi, *J. Electrochem. Soc., 120* (1973) 331.
[5] J.S. Buchanan and L.M. Peter, *Electrochim. Acta, 33* (1988) 127.
[6] D. Pavlov and N. Iordanov, *J. Electrochem. Soc., 117* (1970) 1103.
[7] K. Takashi, N. Hoshihara, H. Yashuda, T. Ishii and H. Jinbo, *J. Power Sources, 30* (1990) 23.
[8] B. Culpin, A.F. Hollenkamp and D.A.J. Rand, *J. Power Sources, 38* (1992) 63–74.
[9] R.F. Nelson and D.M. Wisdom, *J. Power Sources, 33* (1991) 165.
[10] Z. Takehara, K. Kanamura and K. Kawanami, *J. Electrochem. Soc., 137* (1990) 800.
[11] H.K. Giess, in K.R. Bullock and D. Pavlov (eds.), *Proc. Symp. Advances in Lead/Acid Batteries,* Proc. Vol. 84-14, The Electrochemical Society, Pennington, NJ, USA, 1984, p. 241.
[12] P. Simon, N. Bui and F. Dabosi, *J. Power Sources, 50* (1994) 141.
[13] P. Simon, N. Bui, G. Chatainier, M. Provincial and F. Dabosi, *J. Power Sources, 52* (1994) 31.
[14] J.S. Buchanan, N.P. Freestone and L.M. Peter, *J. Electroanal. Chem., 182* (1985) 383.
[15] M.T. Shevalier and V.I. Birss, *J. Electrochem. Soc., 137* (1990) 2643.
[16] M. Pourbaix, *Atlas d'Equilibres Electrochimique à 25 °C,* Gauthier–Villars, Paris, 1963, p. 485.
[17] D. Pavlov, B. Monhakov, M. Maja and N. Penazi, *J. Electrochem. Soc., 136* (1989) 27.
[18] M. Bojinov, K. Salmi and G. Sundholm, *Electrochim. Acta, 39* (1994) 719.
[19] H. Doëring, J. Garche, H. Dietz and K. Wiezener, *J. Power Sources, 30* (1990) 41.
[20] F.E. Varela, L.M. Gassa and J.L. Vilche, *J. Electroanal. Chem., 353* (1993) 147.
[21] S.R. Morisson, *Electrochemistry of Semiconductor and Oxidized Electrodes,* Plenum, New York, 1984.
[22] Z. Stoynov and B. Savova-Stoynova, *Ext. Abstr., First Int. Symp. Electrochemical Impedance Spectroscopy, 22–26 May 1989, Carcans, France,* Abstr. No. C2.9.
[23] M.N.C. Ijomah, *J. Appl. Electrochem., 18* (1988) 142.
[24] J. Garche, *J. Power Sources, 30* (1990) 47.